Patterns in the Lattice Homology of Seifert Homology Spheres

Karthik Seetharaman
Massachusetts Academy of Math and Science at WPI

William Yue
Phillips Academy Andover

Isaac Zhu
North Carolina School of Science and Mathematics

MIT PRIMES Research
Boston, Massachusetts

Under the direction of
Dr. Irving Dai
Stanford University

Patterns in the Lattice Homology of Seifert Homology Spheres

Karthik Seetharaman, William Yue, and Isaac Zhu

September 13, 2021

Abstract

Seifert fibered integral homology spheres are an important class of 3-dimensional manifolds. There are several numerological invariants and properties of these manifolds that are studied, such as the d-invariant and the lattice homology, which have been of intense interest in the last few decades, as well as the maximal monotone subroot, which is a homology cobordism invariant recently introduced by Dai and Manolescu in 2017. In this paper, we prove that the d-invariants of the Seifert homology spheres $\Sigma(a_1, a_2, \ldots, a_n)$ and $\Sigma(a_1, a_2, \ldots, a_{n-1}, a_n + a_1a_2 \cdots a_{n-1})$ are equal using a novel method which analyzes their τ-sequences and the behavior of the numerical semigroup minimally generated by $a_1a_2 \cdots a_n/a_i$ for $i \in [1, n]$. Then, we prove the new result that the maximal monotone subroots of the lattice homologies of $\Sigma(a_1, a_2, \ldots, a_n)$ and $\Sigma(a_1, a_2, \ldots, a_{n-1}, a_n + 2a_1a_2 \cdots a_{n-1})$ are equal. However, we note that the maximal monotone subroots of the lattice homologies of $\Sigma(a_1, a_2, \ldots, a_n)$ and $\Sigma(a_1, a_2, \ldots, a_{n-1}, a_n + a_1a_2 \cdots a_{n-1})$ are in general *not* always equal.

Keywords: lattice homology, Seifert fibered integral homology spheres, homology cobordism group, d-invariant, maximal monotone subroot

Contents

1 Introduction

The concept of cobordism is extremely fundamental in topology. Recall that two smooth n-dimensional manifolds Y_1 and Y_2 are *cobordant* if $-Y_1 \sqcup Y_2$ is the boundary of some smooth $(n+1)$-dimensional manifold W. Cobordisms have been studied extensively for many decades now and have many applications to other areas of topology and mathematics in general (see [3], [7], [20], and [26], all published in this year).

A natural specialization of cobordism exists in low dimensions called *homology cobordism*. An integral homology 3-sphere is a manifold X with the same homology as a 3-sphere; that is, $H_*(X, \mathbb{Z}) = H_*(S^3, \mathbb{Z})$. We define an integral homology 4-ball and an integral homology cylinder similarly, as manifolds with the same homology groups as B^4 and $S^3 \times I$, respectively, where I is a closed interval. Similar to cobordism, we say that two integral homology 3-spheres Y_1 and Y_2 are *homology cobordant* if $-Y_1 \sqcup Y_2$ is the boundary of some homology cylinder. Taking the set of all integral homology 3-spheres, we get a natural group structure under the equivalence relation of homology cobordism, where the operation is connected sum, the identity is S^3, and the inverse of a 3-manifold Y is $-Y$, where $-Y$ denotes Y with its orientation reversed. This group is called the *homology cobordism group* $\Theta^3_{\mathbb{Z}}$. Over the last decades, there has been many attempts to understand this group more fully; for example, it is known that $\Theta^3_{\mathbb{Z}}$ has a $\mathbb{Z}$ summand and contains $\mathbb{Z}^\infty$ as a subgroup; these are Theorems 2.3 and 2.2 respectively in [17]. For more exposition on this as well as other topics in this introduction, we refer the reader to [14] and the aforementioned [17].

Many proofs in the study of the homology cobordism group rely on *Heegaard Floer homology*, an invariant of 3-manifolds defined by Ozsváth and Szabó in [22]. This invariant is quite complicated to define, and we refer the interested reader to [23] for more exposition. It turns out that, for certain classes of manifolds, the Heegaard Floer homology is isomorphic to another combinatorially-defined invariant known as the *lattice homology*, which is easier to understand and compute. One such class of manifolds for which this is true is *Seifert fibered integral homology spheres*, which are an important class of examples in the study of the homology cobordism group (see [5] and [10]). For any n-tuple $a_1, a_2, \ldots, a_n$ of pairwise coprime positive integers that are at least 2, the Seifert fibered integral homology sphere $\Sigma(a_1, a_2, \ldots, a_n)$ is defined by surgery on a link (refer to Subsection 2.1). These manifolds have a lot of nice structure to them, and in particular the 3-fibered case of $\Sigma(p, q, r)$ for pairwise coprime positive integers $p, q, r \geq 2$ has been studied extensively. In the 3-fibered case, Seifert fibered integral homology spheres are known as *Brieskorn spheres*. Brieskorn spheres are also of interest since they can defined as the intersection of a small sphere around the origin with the singular hypersurface $x^p + y^q + z^r = 0$ in $\mathbb{C}^3$ as in [1]. The case of 4 or more fibers, however, has not been studied nearly as extensively.

In this paper, we study the lattice homologies of Seifert fibered integral homology spheres, which can be computed combinatorially using the τ-sequence (refer to Subsection 2.3), which is derived by the numerical semigroup minimally generated by $a_1 a_2 \cdots a_n / a_i$ for $i \in [1, n]$, as in [4]. Though this reformulation is easier to compute, it is still complicated and far from closed-form. There is plenty of interest in computing the lattice homologies of Brieskorn spheres such as in [9], [24], and [27].

In the first part of our paper, we focus on the d-invariants of these spheres. The d-invariant is a numerical invariant derived from Heegaard Floer homology (and thus in our case the lattice homology), of a 3-manifold, and is another important invariant. It turns out that, for the manifolds of interest, the d-invariant can be computed with an understanding of the τ-sequence of the manifold, a sequence used to compute the lattice homologies of Seifert fibered integral homology spheres (refer to Subsection 2.3). In addition, d-invariants are a homology cobordism invariant: if two manifolds Y_1 and Y_2 are homology cobordant, then they have the same d-invariant (see [8]). The d-invariant also specifies a surjective homomorphism from $\Theta^3_{\mathbb{Z}}$ to $2\mathbb{Z}$ as stated in [12].

We prove the following theorem about d-invariants:

Theorem 1.1. *The d-invariants of the two Seifert fibered integral homology spheres*

$$\Sigma(a_1, a_2, \ldots, a_{n-1}, a_n) \qquad \textit{and} \qquad \Sigma(a_1, a_2, \ldots, a_{n-1}, a_n + \alpha)$$

are equal for pairwise relatively prime positive integers $a_1, a_2, \ldots, a_n \geq 2$, where we define $\alpha := a_1 a_2 \cdots a_{n-1}$. We will continue to use this α notation throughout the paper.

Remark 1.2. The result on d-invariants was proven as Proposition 4.1 of [16], but their proof was topological in nature by interpreting the $+\alpha$ term as surgery on a fiber. Our proof sheds much more insight into the structure of the τ-sequence and related Δ-function themselves, and by extension, the full lattice homology. Methods derived from this are very useful for proving our later results on maximal monotone subroots, which are unknown so far in the literature.

The second part of the paper is dedicated to the study of the *maximal monotone subroot* of Seifert homology spheres, which was introduced by [21] recently. The maximal monotone subroot is another homology cobordism invariant that is defined for certain plumbed 3-manifolds, including all Seifert homology spheres, which can be derived from their lattice homology. As there is plenty of interest in understanding the full lattice homology, it is natural to try to understand the maximal monotone subroot as well.

In this paper, we prove the following theorem about the maximal monotone subroots of the lattice homologies of Seifert fibered integral homology spheres.

Theorem 1.3. *The maximal monotone subroots of the lattice homologies of the two Seifert fibered integral homology spheres*

$$\Sigma(a_1, a_2, \ldots, a_n) \qquad \textit{and} \qquad \Sigma(a_1, a_2, \ldots, a_n + 2\alpha)$$

are the same for pairwise relatively prime positive integers $a_1, a_2, \ldots, a_n \geq 2$. Recall that $\alpha := a_1 a_2 \cdots a_{n-1}$.

Very specialized cases of this theorem have been established before. For example, a consequence of Proposition 22.9 of [11] is that the maximal monotone subroots of the lattice homologies of $\Sigma(p, q, pqn \pm 1)$ and $\Sigma(p, q, pq(n+2) \pm 1)$ are the same. In Theorem 1.3, we generalize this result both to an arbitrary number of fibers and for a_n to be an arbitrary residue modulo α (it is not restricted to just $\pm 1 \pmod{\alpha}$).

Remark 1.4. Note that if an integral homology sphere is homology cobordant to S^3, then it bounds an integral homology ball. Since S^3 has a d-invariant of 0 and a trivial maximal monotone subroot (that is, just a single upwards infinite stem), in order for a Seifert fibered integral homology sphere to bound an integral homology 4-ball, its d-invariant must be 0 and its maximal monotone subroot must be trivial.

Remark 1.5. It has been shown in Theorem 2.2 of [17] that the classes $[\Sigma(2, 3, 6k - 1)]$ are linearly independent in $\Theta^3_{\mathbb{Z}}$ (using a different set of invariants). This is in constrast to the d-invariant, which we've shown in Theorem 1.1 to be unable to distinguish any of these classes, and the maximal monotone subroot, which we've shown in Theorem 1.3 to at most be able to distinguish the parity of k.

Here are some corollaries of Theorems 1.1 and 1.3.

Corollary 1.6. *If we know that two Seifert fibered integral homology spheres Y_1 and $Y_2 = \Sigma(a_1, a_2, \ldots, a_{n-1}, a_n)$ are not homology cobordant because their d-invariants are different, then Y_1 and $Y_2' = \Sigma(a_1, a_2, \ldots, a_{n-1}, a_n + \alpha)$ also aren't homology cobordant. Similarly, if we know that Y_1 and Y_2 are not homology cobordant because their maximal monotone subroots are different, then Y_1 and $Y_2'' = \Sigma(a_1, a_2, \ldots, a_{n-1}, a_n + 2\alpha)$ also aren't homology cobordant.*

Corollary 1.7. *Two Seifert fibered integral homology spheres $Y = \Sigma(a_1, a_2, \ldots, a_{n-1}, a_n)$ and $Y' = \Sigma(a_1, a_2, \ldots, a_{n-1}, a_n + \alpha)$ cannot be distinguished in $\Theta^3_{\mathbb{Z}}$ by the d-invariant. Similarly, the two Seifert homology spheres Y and $Y'' = \Sigma(a_1, a_2, \ldots, a_n + 2\alpha)$ cannot be distinguished in $\Theta^3_{\mathbb{Z}}$ by the maximal monotone subroot.*

2 Preliminaries

In this section, we recall the definitions of Seifert fibered integral homology spheres and lattice homology, and then review a method of computing the lattice homology of Seifert homology spheres.

2.1 Seifert fibered integral homology spheres

Definition 2.1. Let $a_1, a_2, \ldots, a_n$ be pairwise coprime positive integers. Solve the equation

$$\sum_{i=1}^{n} \frac{b_i}{a_i} \left(\prod_{j=1}^{n} a_j \right) = -1 - e_0 a_1 a_2 \cdots a_n \tag{1}$$

for $(e_0, b_1, b_2, \ldots, b_n)$, where we restrict $1 \leq b_i < a_i$ for all $i \in [1, n]$. Taking this equation modulo a_i gives

$$\frac{a_1 a_2 \cdots a_n b_i}{a_i} \equiv -1 \pmod{a_i}, \tag{2}$$

so there is a unique solution for each b_i. Note that $e_0 < 0$. Then the *Seifert homology sphere* $\Sigma(a_1, a_2, \ldots, a_n)$ is defined as the generalized Seifert manifold

$$M(e_0, (a_1, b_1), (a_2, b_2), \ldots, (a_n, b_n))$$

over S^2, with surgery diagram shown in Figure 1. Note that equation (1) ensures that this manifold is an integral homology sphere.

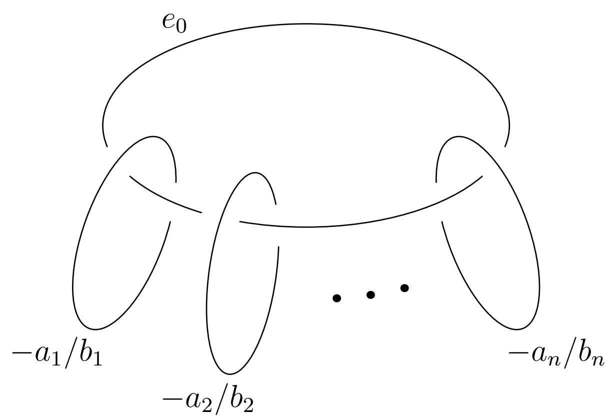

Figure 1: Rational surgery diagram for the Seifert homology sphere $\Sigma(a_1, a_2, \ldots, a_n)$

2.2 Lattice homology

This paper investigates the *lattice homologies* of these Seifert homology spheres. In this section, we define the lattice homology, which is an invariant defined for plumbed 3-manifolds together with a chosen equivalence class of characteristic vector (refer to Definitions 2.4 and 2.5). Though the exact details of the definition of lattice homology will be unnecessary for understanding the rest of the paper, we include them for completeness.

Definition 2.2. A *plumbed 3-manifold* is a manifold with a surgery diagram consisting of integral surgeries on unknots linked together in a tree.

To define lattice homology, we use the *plumbing graph* of a plumbed 3-manifold Y, which is a decorated tree that represents the integral surgery diagram of Y, created by replacing each unknot with a vertex and connecting an edge between vertices if their respective unknots are linked. For the particular case of Seifert homology spheres $\Sigma(a_1, a_2, \ldots, a_n)$, we can obtain this by replacing each rational surgery in Figure 1 with a chain of unknots with coefficients determined by partial fraction decomposition; the integral surgery diagram and plumbing graph of $\Sigma(a_1, a_2, \ldots, a_n)$ is shown in Figure 2. The definition of lattice homology requires that the manifold admits a negative-definite plumbing graph, and for the rest of this section, we will assume that all plumbing graphs are negative-definite.

Definition 2.3. The *intersection form* $(-,-)$ of a given plumbing graph Γ of a plumbed 3-manifold Y is defined on the lattice $L_\Gamma = \mathrm{Span}_{\mathbb{Z}}(v_1, v_2, \ldots, v_n)$ formally spanned by the vertices $v_1, v_2, \ldots, v_n$ of Γ. It is given by

$$(v_i, v_j) = \begin{cases} 0 & i \neq j \text{ and } v_i, v_j \text{ not adjacent} \\ 1 & i \neq j \text{ and } v_i, v_j \text{ adjacent} \\ \text{decoration of } v_i & i = j \end{cases},$$

which is then extended bilinearly to all of $L_\Gamma \otimes \mathbb{Q}$. Note that this is just the adjacency matrix of Γ, except vertices have a self-adjacency equal to their decoration.

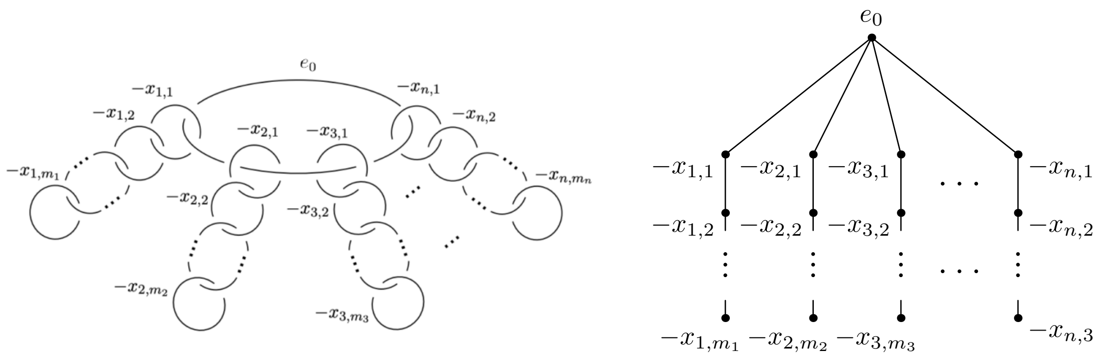

Figure 2: Integral surgery diagram (on left) and associated plumbing graph (on right) of Seifert homology sphere $\Sigma(a_1, a_2, \cdots, a_n)$, where the partial fraction decomposition of $\frac{a_i}{b_i}$ is $[x_{i,1}, x_{i,2}, \ldots, x_{i,m_i}]$ for each $i \in [1, n]$.

Definition 2.4. Let k be an element of the rational lattice $L_\Gamma \otimes \mathbb{Q}$. We say k is a *characteristic vector* if

$$(k, x) \equiv (x, x) \pmod 2$$

for all $x \in L_\Gamma$. The set of characteristic vectors is denoted as Char_Γ.

Definition 2.5. Given any characteristic vector $k \in \mathrm{Char}_\Gamma$ and element $y \in L_\Gamma$, the vector $k + 2y$ is also characteristic. This action of L_Γ partitions the set of characteristic vectors into equivalence classes, and we denote the equivalence class of k by $[k]$.

We can now define lattice homology as in [19], which is an invariant of a plumbed 3-manifold along with a chosen equivalence class of characteristic vector. We will do so using sublevel sets. Let Γ be any plumbing graph and fix $k \in \mathrm{Char}_\Gamma$. We define a weight function

$$w(x) = \frac{(x, x) + (k, x)}{2}$$

and extend it to d-dimensional cubes of side-length one by setting

$$w(x_d) = \min_{x \text{ a vertex of } x_d} w(x),$$

where x_d is an d-dimensional cube. For any n, the *sublevel set* S_n is defined as

$$S_n = \bigcup_{w(y) \geq n} y,$$

where y is any d-dimensional cube with side length one. We then have the following:

Definition 2.6. Fix a plumbing graph Γ for a plumbed 3-manifold Y, and for each $n \in \mathbb{Z}$, draw a vertex for each connected component in the sublevel set S_n at height $-2n$ on the page. Note that $S_{n+1} \subseteq S_n$ for all $n \in \mathbb{Z}$, so for each n define the map $T_n : S_{n+1} \to S_n$ that sends each connected component in S_{n+1} to the one it is contained in inside S_n. Record the results of this map by drawing lines between corresponding vertices in the diagram. This gives a *graded root*, as shown in Figure 3. The lattice homology is this graded root with all heights shifted by the quantity $-\frac{(k,k)+|\Gamma|}{4}$; note that the final height of each vertex is called its *grading*.

Figure 3: The plumbing graph of $\Sigma(2,3,7)$ on the left with its graded root lattice homology on the right.

Note that since the sublevel sets consist of the d-dimensional cubes with side length one contained within some expanding ellipsoid, there will eventually be only one connected component for all sufficiently negative n. This corresponds to the infinite tower on top of the lattice homology. On the other hand, when n is larger than the maximum of the weight function on the intersection form, S_n contains no connected components, which corresponds to the lattice homology ending when it's sufficiently low.

Remark 2.7. Remarkably, it can be shown that, up to equivalence classes of characteristic vectors, the lattice homology does not depend on the particular plumbing diagram chosen for a plumbed 3-manifold; that is, it is an invariant of plumbed 3-manifolds themselves. Note, however, that while lattice homology does not depend on the specific characteristic vector in a chosen equivalence class, it does vary if a different equivalence class of characteristic vectors is chosen.

As stated in [21], every Seifert homology sphere has a negative-definite plumbing graph, and thus a lattice homology. Furthermore, because they are integral homology spheres, it turns out that these manifolds only admit one equivalence class of characteristic vector anyway, so each only has one lattice homology. It is also known that, for certain plumbed 3-manifolds with negative-definite plumbing (such as integral Seifert homology spheres), the lattice homology is isomorphic to the Heegaard-Floer homology [21], a long-studied and important invariant whose definition is outside the scope of this paper.

We can now define the d-invariant of a 3-manifold, as in [13].

Definition 2.8. The *d-invariant* of a 3-manifold is -1 times the grading of the lowest vertex of its lattice homology.

Remark 2.9. The factor of -1 is simply for convention reasons.

2.3 Constructing the lattice homology of Seifert homology spheres using the τ-sequence

As it turns out, for Seifert homology spheres, the lattice homology and d-invariant can be understood through the behavior of a particular sequence known as the τ-sequence.

Definition 2.10. Consider a Seifert homology sphere $\Sigma(a_1, a_2, \dots, a_n)$. The *τ-sequence* is defined by the recurrence

$$\tau(x+1) = \tau(x) + 1 + |e_0|x - \sum_{i=1}^{n} \left\lceil \frac{xb_i}{a_i} \right\rceil,$$

where, as before,

$$\sum_{i=1}^{n} \frac{b_i}{a_i} \left(\prod_{j=1}^{n} a_j \right) = -1 - e_0 a_1 a_2 \dots a_n.$$

Definition 2.11. We define the difference term in the above recurrence as the Δ*-function*

$$\Delta(x) = 1 + |e_0|x - \sum_{i=1}^{n} \left\lceil \frac{xb_i}{a_i} \right\rceil.$$

Therefore,

$$\tau(x) = \sum_{i=0}^{x-1} \Delta(i).$$

Now, we review a method of computing the lattice homology of Seifert homology spheres using this τ-sequence.

Definition 2.12. We say that $\tau(M)$ is a *local maximum* of τ if there exists integers α, β with $\alpha < M < \beta$ such that $\tau(\alpha) < \tau(M) > \tau(\beta)$, and τ is monotone nondecreasing on the interval $[\alpha, M]$ and monotone nonincreasing on the interval $[M, \beta]$. *Local minimum* values $\tau(m)$ are defined analogously. Together, these are called the *local extrema* of τ.

Definition 2.13. Consider the sequence of all local extrema of the τ-sequence. However, sometimes the τ-sequence remains constant at a local extrema for multiple consecutive inputs. We choose to count these consecutive repeated local extrema as a single value. For example, the sequence $[0, 1, 1, 1, -1, -1, 1, 1, 1, 0]$ of all local extrema (including consecutive repeated ones) of τ is collapsed into $[0, 1, -1, 1, 0]$. This collapsed sequence, denoted τ_{ex}, and is called the *τ-extrema sequence*.

We can associate τ_{ex} with a graded root, which, after a grading shift, gives the lattice homology of the Seifert homology sphere. For any graded root, we can associated it to a sequence through the following procedure: given any graded root, we consider a path that wraps around the tree, starting to the left of the infinite stem and ending to its right. As an example, in Figure 4, the path is drawn in blue.

Then, we mark every local minimum of this blue path with a red point and every local maximum of this blue path with a green point; more formally, red points are where the blue path changes from moving downwards to moving upwards, and green points are where the blue path changes from moving upwards to moving downwards. Recording the gradings of the vertices of the graded root where these local extrema occur in order along the blue path gives the sequence associated to this graded root. In the example in Figure 4, we get the sequence $[0, 2, 0, 1, -1, 1, 0, 2, 0]$. In general, this procedure gives some sequence

$$[m_1, M_1, m_2, M_2, \dots, m_{n-1}, M_{n-1}, m_n]$$

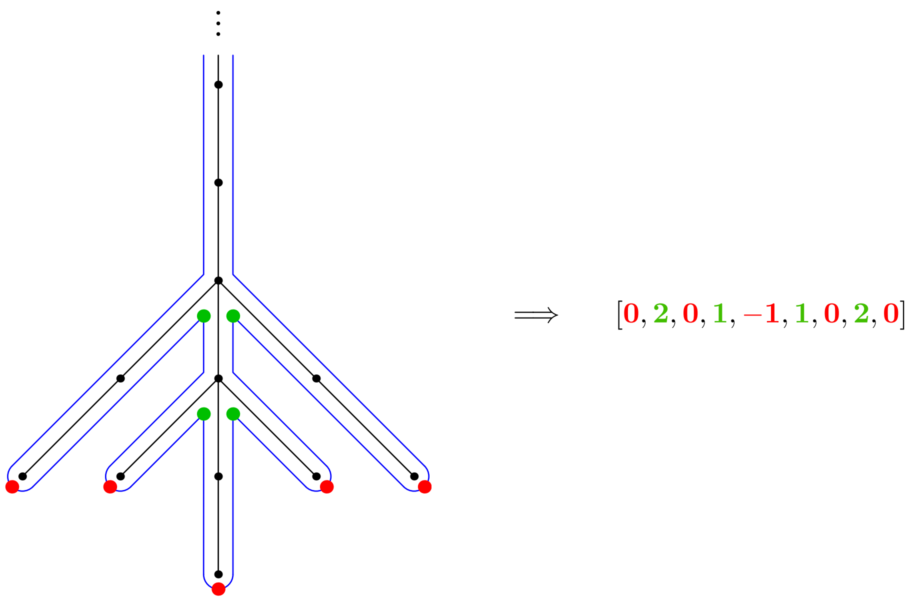

Figure 4: Example of extracting sequence from graded root, assuming the grading of the leftmost vertex is 0.

of numbers such that $M_i > \max\{m_i, m_{i+1}\}$ for $i = 1, 2, \ldots, n-1$. Conversely, any such sequence s also uniquely corresponds to a graded root, which we denote by R_s.

Since $2\tau_{\text{ex}}$ is a sequence of alternating local minima and maxima, it has an associated graded root $R_{2\tau_{\text{ex}}}$. It turns out that this graded root, after a global grading shift, matches the lattice homology of the Seifert homology sphere. Note that the factor of 2 ensures that all gradings are the same parity, as in the lattice homology.

Theorem 2.14 ([18])**.** *The lattice homology of the Seifert homology sphere $\Sigma(a_1, a_2, \ldots, a_n)$ is isomorphic to $R_{2\tau_{ex}}$ after applying a global grading shift $-\frac{K^2+|\Gamma|}{4}$, where K is the canonical cohomology class, which can be viewed as a specially selected characteristic vector.*

Remark 2.15. It turns out that the graded root $R_{2\tau_{\text{ex}}}$ is symmetric (which is required since the lattice homology is necessarily symmetric by definition). This is true because of Property 2 of Theorem 3.1.

3 Properties of the τ-Sequence and Δ-Function

In this section we will develop a pictorial representation of the Δ-function, by constructing a table of the integers with $\alpha := a_1 a_2 \cdots a_{n-1}$ columns. This picture will be critical to our later analysis. Figure 5 depicts the function for $(a_1, a_2, a_3) = (3, 7, 29)$, where the width of the grid is $3 \cdot 7 = 21$.

Let $\Delta : \mathbb{Z} \to \mathbb{Z}$ be given by

$$\Delta(x) = 1 + |e_0|x - \sum_{i=1}^{n} \left\lceil \frac{x b_i}{a_i} \right\rceil$$

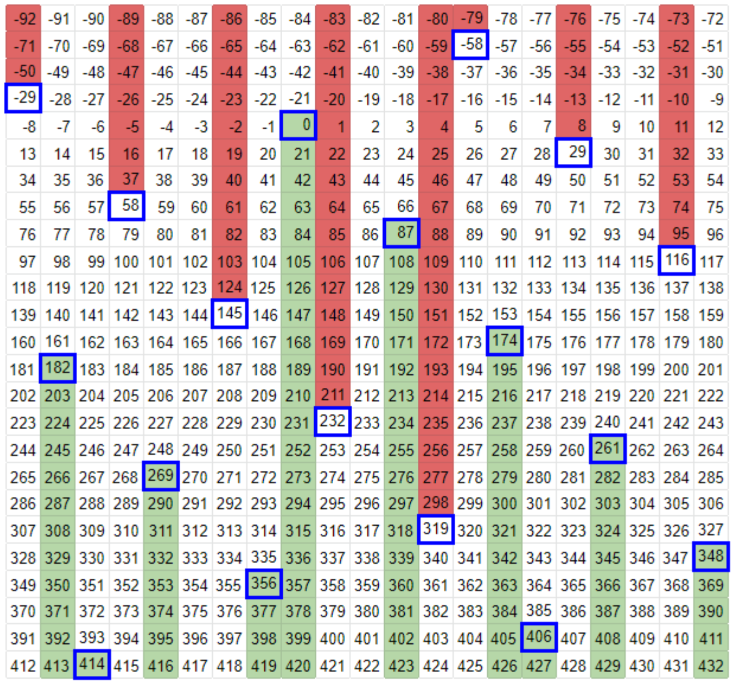

Figure 5: This diagram represents the Δ-function pictorally, and it displays information for $(p, q, r) = (3, 7, 29)$ with some arbitrarily chosen bounds. As we will soon see, the blue bordered boxes are multiples of a_n, the green boxes have $\Delta(x) = 0$, the red boxes have $\Delta(x) = -1$, and the white boxes have $\Delta(x) = 0$. As some random examples, $\Delta(-44) = -1$, $\Delta(145) = 1$, and $\Delta(339) = 1$.

for all $x \in \mathbb{Z}$. With this consideration of domain, we have the following natural extension of Theorem 4.1 in [4]:

Theorem 3.1. *Let $a_1, a_2, \ldots, a_n$ be pairwise relatively prime positive integers, and define*

$$\Delta(x) = 1 + |e_0|x - \sum_{i=1}^{n} \left\lceil \frac{xb_i}{a_i} \right\rceil,$$

as before. Define the constant

$$N_0 = a_1 a_2 \cdots a_n \left((n-2) - \sum_{i=1}^{n} \frac{1}{a_i} \right) \in \mathbb{Z}_{>0}.$$

Then, the following properties hold:

1. $\Delta(x) \geq 0$ *for all* $x > N_0$.
2. $\Delta(x) = -\Delta(N_0 - x)$ *for* all $x \in \mathbb{Z}$.
3. *For* all $x \in \mathbb{Z}$, *one has* $\Delta(x) \geq 1$ *if and only if* x *is an element of the numerical semigroup* G *minimally generated by* $a_1 a_2 \cdots a_n / a_i$ *for* $i \in [1, n]$ *(defined below in Definition 3.2).*

4. If $x \in G$ *and* $x = a_1a_2\cdots a_n \sum_{i=1}^{n} \frac{x_i}{a_i}$*, then* $\Delta(x) = 1 + \sum_{i=1}^{n} \left\lfloor \frac{x_i}{a_i} \right\rfloor$.

Definition 3.2. The numerical semigroup G minimally generated by $a_1a_2\cdots a_n/a_i$ for $i \in [1, n]$ is the set of all $x \in \mathbb{Z}$ that can be expressed as a nonnegative integer linear combination of $a_1a_2\cdots a_n/a_i$. That is,

$$G = \left\{ x \in \mathbb{Z} : x = a_1a_2\cdots a_n \sum_{i=1}^{n} \frac{x_i}{a_i} \text{ for some } x_i \in \mathbb{Z}_{\geq 0} \right\}.$$

Remark 3.3. Note that since $\Delta(x) \geq 0$ for all $x > N_0$, and Property 2 of Theorem 3.1 gives that $\Delta(x) \leq 0$ for all $x < 0$, the τ-sequence has no local extrema outside of the interval $[0, N_0]$, so this interval is all that matters for constructing the lattice homology.

Let H denote the numerical semigroup minimally generated by the numbers α/a_i for $1 \leq i \leq n-1$.

Lemma 3.4. *If* $s \in H$ *but* $s - \alpha \notin H$*, then* $\Delta(sa_n) = 1$.

Proof. Since $s \in H$, there are nonnegative integers x_i such that

$$sa_n = \left(\alpha \sum_{i=1}^{n-1} \frac{x_i}{a_i} \right) a_n = a_1a_2\cdots a_n \sum_{i=1}^{n-1} \frac{x_i}{a_i}.$$

Notice that we must have $x_i < a_i$ for each i: otherwise, we would have $s - \alpha \in H$. So by Theorem 3.1 we have

$$\Delta(sa_n) = 1 + \sum_{i=1}^{n} \left\lfloor \frac{x_i}{a_i} \right\rfloor = 1.$$

□

We now describe the relationship between the Δs of vertically adjacent cells in the grid (note that x and $x + \alpha$ are vertically adjacent):

Lemma 3.5. *We have that*

$$\Delta(x+\alpha) = \begin{cases} \Delta(x) + 1 & \text{if } a_n \mid x + \alpha \\ \Delta(x) & \text{otherwise} \end{cases}.$$

Proof. We apply the definition of Δ to get

$$\begin{aligned} \Delta(x+\alpha) - \Delta(x) &= |e_0|\alpha - \sum_{i=1}^{n} \left(\left\lceil \frac{(x+\alpha)b_i}{a_i} \right\rceil - \left\lceil \frac{xb_i}{a_i} \right\rceil \right) \\ &= -e_0\alpha - \sum_{i=1}^{n-1} \frac{\alpha b_i}{a_i} - \left\lceil \frac{(x+\alpha)b_n}{a_n} \right\rceil + \left\lceil \frac{xb_n}{a_n} \right\rceil. \end{aligned}$$

Equation (1) gives

$$e_0\alpha = -\frac{1}{a_n} - \sum_{i=1}^{n-1} \frac{\alpha b_i}{a_i} - \frac{\alpha b_n}{a_n},$$

so

$$\Delta(x+\alpha) - \Delta(x) = \frac{1+\alpha b_n}{a_n} - \left\lceil \frac{(x+\alpha)b_n}{a_n} \right\rceil + \left\lceil \frac{xb_n}{a_n} \right\rceil.$$

Now, define the function $\psi(x) := \lceil x \rceil - x$. Plugging this in gives

$$\Delta(x+\alpha) - \Delta(x) = \frac{1}{a_n} - \psi\left(\frac{(x+\alpha)b_n}{a_n}\right) + \psi\left(\frac{xb_n}{a_n}\right).$$

By equation (2), we have that $\alpha b_n \equiv -1 \pmod{a_n}$. Since $\psi(x+k) = \psi(x)$ for all $k \in \mathbb{Z}$, we have

$$\Delta(x+\alpha) - \Delta(x) = \frac{1}{a_n} + \psi\left(\frac{xb_n}{a_n}\right) - \psi\left(\frac{xb_n - 1}{a_n}\right).$$

This quantity equals 1 if and only if $xb_n - 1 \equiv 0 \pmod{a_n}$; in all other cases, it equals 0. However, $xb_n - 1 \equiv 0 \pmod{a_n}$ is equivalent to $x \equiv -\alpha \pmod{a_n}$. Therefore, $\Delta(x+\alpha) - \Delta(x)$ equals 1 if $a_n \mid x + \alpha$ and 0 otherwise, as desired. □

Recalling that $x + \alpha$ is the number directly below x in the grid, this lemma states that as we move downwards in a column, Δ stays the same, unless we reach a multiple of a_n, in which case Δ increases by 1. Combined with Lemma 3.4, we now have the following complete pictorial description of the Δ-function:

- We give every multiple of a_n a blue border. If a blue bordered box sa_n has $s \in H$ and $s - \alpha \notin H$, then we call that box *primitive*. Lemma 3.4 says the Δ-function on primitive boxes evaluates to 1.
- Note there is exactly one primitive blue box in each column: sa_n being in any particular column is equivalent to s being a particular residue modulo α. There is exactly one minimal element of H within any residue class modulo α.
- As we move downwards in a column, the value of Δ stays the same, unless we reach a multiple of a_n, in which case Δ increases by 1.

Figure 6 is an image of the grid for $(a_1, a_2, a_3) = (3, 7, 29)$. The actual integers in each cell have been removed. The blue borders mark multiples of $a_3 = 29$, and the primitive blue boxes are those at the top of the light green columns.
Finally, we introduce the notation

$$\chi(x) := \tau(x) - \tau(x-\alpha) = \Delta(x-\alpha) + \cdots + \Delta(x-1)$$

for all $x \in \mathbb{Z}$.

Lemma 3.6. *For all x, we have*

$$\chi(x+1) - \chi(x) = \begin{cases} 1 & \text{if } x \text{ is a multiple of } a_n \\ 0 & \text{otherwise} \end{cases}.$$

Proof. Note that $\chi(x+1) - \chi(x) = \Delta(x) - \Delta(x-\alpha)$. The result follows from Lemma 3.5. □

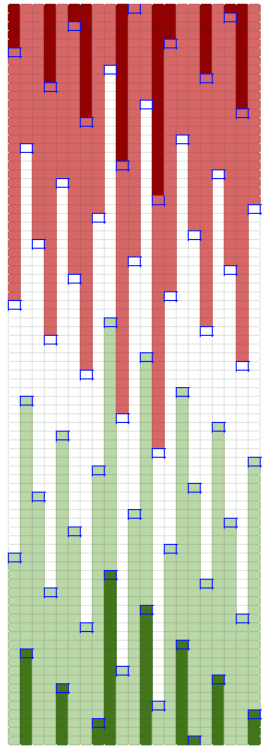

Figure 6: Zoomed-out image of Δ-function for $\Sigma(3, 7, 29)$ without labels in boxes. White cells mean $\Delta = 0$, light green means $\Delta = 1$, dark green means $\Delta = 2$, light red means $\Delta = -1$, and dark red means $\Delta = -2$.

4 Results on d-Invariants

In this section, we prove the following theorem.

Theorem 4.1. *The d-invariants of the Seifert homology spheres $Y = \Sigma(a_1, a_2, \ldots, a_n)$ and $Y' = \Sigma(a_1, a_2, \ldots, a_n + \alpha)$ are equal for all pairwise relatively prime positive integers $a_1, a_2, \ldots, a_n$.*

In order to do this, we will use the following computational formula from [2].

Theorem 4.2. *The d-invariant of a Seifert homology sphere can be computed as*

$$d(Y) = d(\Sigma(a_1, a_2, \ldots, a_n)) = \frac{1}{4}\left(\varepsilon^2 e + e + 5 - 12\sum_{i=1}^{n} s(b_i, a_i)\right) - 2\min_{x\geq 0} \tau_Y(x),$$

where, recall, $(e_0, b_1, b_2, \ldots, b_n)$ satisfy

$$e_0 P + P\sum_{i=1}^{n} \frac{b_i}{a_i} = -1 \tag{3}$$

with $1 \le b_i < a_i$ *for all* $i \in [1, n]$*, where* $P = \prod_{i=1}^n a_i$*. We also define*

$$e = e_0 + \sum_{i=1}^n \frac{b_i}{a_i} \text{ and } \varepsilon = \frac{1}{e}\left(-(n-2) + \sum_{i=1}^n \frac{1}{a_i}\right).$$

Note that τ_Y *is the* τ*-sequence for* Y *and that* $s(b_i, a_i)$ *is a Dedekind sum, given by the formula*

$$s(h,k) := \sum_{i=1}^{k-1} \left\langle \frac{i}{k} \right\rangle \left\langle \frac{hi}{k} \right\rangle,$$

where $\langle \bullet \rangle$ *is the sawtooth function*

$$\langle x \rangle := \begin{cases} 0 & x \in \mathbb{Z} \\ x - \lfloor x \rfloor - \frac{1}{2} & x \notin \mathbb{Z} \end{cases}.$$

Also note that the first term in the d*-invariant formula is precisely the global grading shift* $\frac{K^2 + |\Gamma|}{4}$ *for the canonical cohomology class* K*.*

There are two main components to the formula for the d-invariant in Theorem 4.2: the first term, which is ultimately some function of $a_1, a_2, \ldots, a_{n-1}$; and the second term, which depends on the τ sequence for Y.

4.1 Calculating the required difference in global minima of τ-sequences

To show that $d(Y') - d(Y) = 0$, we start by computing the difference in the first terms to reduce it to a problem in finding the difference in the global minima of τ_Y and $\tau_{Y'}$.

Lemma 4.3. *To prove Theorem 4.1, it is equivalent to demonstrate that*

$$\min_{x \ge 0} \tau_{Y'}(x) - \min_{x \ge 0} \tau_Y(x) = -\frac{1}{8}\left(\left((n-2)\frac{P}{a_n} - \sum_{i=1}^{n-1} \frac{P}{a_n a_i}\right)^2 - 1\right).$$

Note that the right hand side is only a function of $a_1, a_2, \ldots, a_{n-1}$*.*

Dividing both sides of equation (3) in the statement of Theorem 4.2 by P gives $e = -\frac{1}{P}$, so $\varepsilon = (n-2)P - \sum_{i=1}^n \frac{P}{a_i}$. We now plug these into our equation for the d-invariant given by the theorem to get

$$d(Y) = \frac{1}{4}\left(\underbrace{-\left((n-2)P - \sum_{i=1}^n \frac{P}{a_i}\right)^2 \cdot \frac{1}{P}}_{d_1(Y)} \underbrace{- \frac{1}{P} + 5 - 12\sum_{i=1}^n s(b_i, a_i)}_{d_2(Y)}\right) - 2\min_{x \ge 0} \tau_Y(x).$$

Define $d_1(Y)$ and $d_2(Y)$ as above, so that $d(Y) = \frac{1}{4}(-d_1(Y) + d_2(Y)) - 2\min_{x \ge 0} \tau_Y(x)$. Now, note that

$$d_1(Y) = -(n-2)^2 P - \sum_{i=1}^n \frac{P}{a_i^2} - \sum_{1 \le i < j \le n} \frac{2P}{a_i a_j} + \sum_{i=1}^n \frac{2(n-2)P}{a_i}.$$

We will consider the $d_2(Y)$ and $-2\min_{x\geq 0}\tau_Y(x)$ terms later. We now perform the same d-invariant computation for the Brieskorn sphere $Y' = \Sigma(a_1, a_2, \dots, a_{n-1}, a_n + \frac{P}{a_n})$. In what follows, let $a_n' = a_n + \frac{P}{a_n}$ and $P' = \frac{Pa_n'}{a_n}$. Similarly to the previous sphere,

$$d(Y') = \frac{1}{4}\left(\varepsilon'^2 e' + e' + 5 - 12\sum_{i=1}^{n-1} s(b_i', a_i) - 12 s(b_n', a_n')\right) - 2\min_{x\geq 0}\tau_{Y'}(x),$$

where $(e_0', b_1', b_2', \dots, b_{n-1}', b_n')$ satisfy

$$e_0'P' + P'\left(\sum_{i=1}^{n-1}\frac{b_i'}{a_i} + \frac{b_n'}{a_n'}\right) = -1,$$

with $b_i \in [1, a_i - 1]$ for all $1 \leq i \leq n-1$ and $B \in [1, A-1]$. Also, as before, we have

$$e' = e_0' + \sum_{i=1}^{n-1}\frac{b_i'}{a_i} + \frac{b_n'}{a_n'} \text{ and } \varepsilon' = \frac{1}{e'}\left(-(n-2) + \sum_{i=1}^{n-1}\frac{1}{a_i} + \frac{1}{a_n'}\right).$$

Thus, we have $e' = -\frac{1}{P'}$ and $\varepsilon' = (n-2)P' - \sum_{i=1}^{n-1}\frac{P'}{a_i} - \frac{P'}{a_n'}$. Substituting, we have

$$d(Y') = \frac{1}{4}\left(\underbrace{-\left((n-2)P' - \sum_{i=1}^{n-1}\frac{P'}{a_i} - \frac{P'}{a_n'}\right)^2\frac{1}{P'}}_{d_1(Y')}\underbrace{-\frac{1}{P'} + 5 - 12\sum_{i=1}^{n-1}s(b_i', a_i) - 12s(b_n', a_n')}_{d_2(Y')}\right)$$
$$-2\min_{x\geq 0}\tau_{Y'}(x).$$

Once again, we define $d_1(Y')$ and $d_2(Y')$ in such a way that $d(Y') = \dfrac{1}{4}(d_1(Y') + d_2(Y')) - 2\min_{x\geq 0}\tau_{Y'}(x)$. Again, we expand the first term inside the parentheses to get

$$d_1(Y') = -(n-2)^2P' - \sum_{i=1}^{n-1}\frac{P'}{a_i^2} - \frac{P'}{a_n'^2} - \sum_{1\leq i<j\leq n-1}\frac{2P'}{a_ia_j} - \sum_{i=1}^{n-1}\frac{2P'}{a_n'a_i} + \sum_{i=1}^{n-1}\frac{2(n-2)P'}{a_i} + \frac{2(n-2)P'}{a_n'}.$$

We now compute $d_1(Y') - d_1(Y)$. We make heavy use of the identities $a_n' - a_n = \frac{P}{a_n}$, $P' - P = \frac{P^2}{a_n^2}$, and $\frac{P'}{a_n'} = \frac{P}{a_n}$ to eliminate all occurrences of a_n' and P' from this difference. All of these identities are easily verified from the definitions of a_n' and P'. With some computation, the difference comes out to:

$$d_1(Y') - d_1(Y) = -(n-2)^2\cdot\frac{P^2}{a_n^2} - \sum_{i=1}^{n-1}\frac{P^2}{a_n^2a_i^2} + \frac{P^2}{a_n^2}\cdot\frac{1}{a_n'a_n} - \sum_{1\leq i<j\leq n-1}\frac{2P^2}{a_n^2a_ia_j} + \sum_{i=1}^{n-1}\frac{2(n-2)P^2}{a_n^2a_i}.$$

We can also evaluate the second difference term as

$$d_2(Y') - d_2(Y) = \frac{1}{P} - 5 + 12\sum_{i=1}^{n} s(b_i, a_i) - \frac{1}{P'} + 5 - 12\sum_{i=1}^{n-1} s(b'_i, a_i) + 12s(b'_n, a'_n)$$
$$= \frac{1}{a'_n a_n} + 12s(b_n, a_n) - 12s(b'_n, a'_n).$$

The final simplification is due to the fact that $b'_i = b_i$ for all $1 \le i \le n-1$, which is true by equation (2).

To evaluate this, we use the following facts about Dedekind sums from [25]:

- $s(h,k) = -s(-h,k)$.
- If $h_1 \equiv h_2 \pmod{k}$, then $s(h_1,k) = s(h_2,k)$.
- When $h_1 h_2 \equiv 1 \pmod{k}$, $s(h_1,k) = s(h_2,k)$.
- $s(h,k) = -\frac{1}{4} + \frac{1}{12}\left(\frac{h}{k} + \frac{k}{h} + \frac{1}{kh}\right) - s(k,h)$ (The Dedekind Reciprocity Law).

Recall that $b_n \equiv -\frac{1}{a_1 a_2 \cdots a_{n-1}} \pmod{a_n}$. Similarly, $b'_n \equiv -\frac{1}{a_1 a_2 \cdots a_{n-1}} \pmod{a'_n}$. Thus,

$$\begin{aligned} s(b_n, a_n) &= s(-a_1 a_2 \cdots a_{n-1}, a_n) \\ &= -s(a_1 a_2 \cdots a_{n-1}, a_n) \\ &= \frac{1}{4} - \frac{1}{12}\left(\frac{a_1 a_2 \cdots a_{n-1}}{a_n} + \frac{a_n}{a_1 a_2 \cdots a_{n-1}} + \frac{1}{a_1 a_2 \cdots a_n}\right) + s(a_n, a_1 a_2 \dots a_{n-1}), \end{aligned}$$

where we use the Dedekind Reciprocity Law. Similarly,

$$s(b'_n, a'_n) = \frac{1}{4} - \frac{1}{12}\left(\frac{a_1 a_2 \dots a_{n-1}}{a'_n} + \frac{a'_n}{a_1 a_2 \dots a_{n-1}} + \frac{1}{a_1 a_2 \dots a_{n-1} a'_n}\right) + s(a'_n, a_1 a_2 \dots a_{n-1}).$$

Subtracting, we get

$$\begin{aligned} 12s(b_n, a_n) - 12s(b'_n, a'_n) = &\frac{a_1 a_2 \cdots a_{n-1}}{a'_n} + \frac{a'_n}{a_1 a_2 \cdots a_{n-1}} + \frac{1}{a_1 a_2 \cdots a_{n-1} a'_n} \\ &- \frac{a_1 a_2 \cdots a_{n-1}}{a_n} - \frac{a_n}{a_1 a_2 \cdots a_{n-1}} - \frac{1}{a_1 a_2 \cdots a_n}. \end{aligned}$$

Using the identity $a'_n - a_n = a_1 a_2 \cdots a_{n-1}$, we get

$$12s(b_n, a_n) - 12s(b'_n, a'_n) = \frac{-(a_1 a_2 \cdots a_{n-1})^2 + a'_n a_n - 1}{a'_n a_n}$$

after a bit of computation. Thus, we have:

$$\begin{aligned} d(Y') - d(Y) = \frac{1}{4}\Bigg(&-(n-2)^2\left(\frac{P^2}{a_n^2}\right) - \sum_{i=1}^{n-1}\frac{P^2}{a_n^2 a_i^2} + \frac{P^2}{a_n^2}\left(\frac{1}{a'_n a_n}\right) - \sum_{1 \le i < j \le n-1}\frac{2P^2}{a_n^2 a_i a_j} \\ &+ \sum_{i=1}^{n-1}\frac{2(n-2)P^2}{a_n^2 a_i} + \frac{1}{a'_n a_n} + \frac{-(a_1 a_2 \cdots a_{n-1})^2 + a'_n a_n - 1}{a'_n a_n}\Bigg) + 2\min_{x \ge 0}\tau_Y(x) - 2\min_{x \ge 0}\tau_{Y'}(x). \end{aligned}$$

For the d-invariants to be equal, we must have

$$\min_{x\geq 0}\tau_{Y'}(x)-\min_{x\geq 0}\tau_{Y}(x)=\frac{1}{8}\Bigg(-(n-2)^2\left(\frac{P^2}{a_n^2}\right)-\sum_{i=1}^{n-1}\frac{P^2}{a_n^2a_i^2}+\frac{P^2}{a_n^2}\left(\frac{1}{a_n'a_n}\right)$$
$$-\sum_{1\leq i<j\leq n-1}\frac{2P^2}{a_n^2a_ia_j}+\sum_{i=1}^{n-1}\frac{2(n-2)P^2}{a_n^2a_i}+\frac{1}{a_n'a_n}+\frac{-(a_1a_2\cdots a_{n-1})^2+a_n'a_n-1}{a_n'a_n}\Bigg).$$

Note that $-(a_1a_2\cdots a_{n-1})^2=-\frac{P^2}{a_n^2}$, so the $\frac{P^2}{a_n^2}\left(\frac{1}{a_n'a_n}\right)$ and $-\frac{(-a_1a_2\cdots a_{n-1})^2}{a_n'a_n}$ cancel. Additionally, the $\frac{1}{a_n'a_n}$ and $-\frac{1}{a_n'a_n}$ terms cancel, so that we are left with

$$\min_{x\geq 0}\tau_{Y'}(x)-\min_{x\geq 0}\tau_{Y}(x)=\frac{1}{8}\Bigg(-(n-2)^2\left(\frac{P^2}{a_n^2}\right)-\sum_{i=1}^{n-1}\frac{P^2}{a_n^2a_i^2}-\sum_{1\leq i<j\leq n-1}\frac{2P^2}{a_n^2a_ia_j}$$
$$+\sum_{i=1}^{n-1}\frac{2(n-2)P^2}{a_n^2a_i}+1\Bigg).$$

The expression inside the parentheses factors into

$$1-\left((n-2)\frac{P}{a_n}-\sum_{i=1}^{n-1}\frac{P}{a_na_i}\right)^2,$$

which can be checked manually by expansion. This gives the desired result. □

Surprisingly, this quantity is tied to the numerical semigroup generated by the $n-1$ elements $\frac{\alpha}{a_i}$ for $i\in[0,n-1]$, as we will now show.

Lemma 4.4. *For pairwise relatively prime positive integers $a_1,a_2,\ldots,a_n$ where we define $P:=a_1a_2\cdots a_n$, the largest positive integral nonelement of the numerical semigroup G minimally generated by $\frac{P}{a_i}$ for $i\in[1,n]$ is precisely*

$$(n-1)P-\sum_{i=1}^{n}\frac{P}{a_i}.$$

Proof. As before, let $\alpha=\frac{P}{a_n}$ and consider the semigroup H minimally generated by the set $\{\frac{\alpha}{a_i}\}_{i\in[1,n-1]}$, and let a_nH be the set when all elements are multiplied by a_n. Consider arranging the natural numbers in an infinite table, with columns corresponding to residues modulo α, similar to the grid in Section 3. Color elements of H purple. Any term in the table on or below a purple term in the same column will be in G. This is because all elements of G can be expressed as some element of a_nH plus some nonnegative multiple of α, which corresponds to shifting downwards in the same column. Thus, it suffices to find the largest purple term with no purple terms above it, and subtract α from it.

Every purple term can be written in the form $a_n\sum_{i=1}^{n-1}\frac{c_i\alpha}{a_i}$ for some nonnegative integers $c_1,c_2,\ldots,c_{n-1}$. Now, note that two purple terms $a_n\sum_{i=1}^{n-1}\frac{c_i\alpha}{a_i}$ and $a_n\sum_{i=1}^{n-1}\frac{d_i\alpha}{a_i}$ are equal if and only if

$$P\sum_{i=1}^{n-1}\frac{c_i}{a_i} \equiv P\sum_{i=1}^{n-1}\frac{d_i}{a_i} \pmod{\alpha}.$$

Since both sides are equivalent modulo a_1, we must have $\frac{c_1 P}{a_1} \equiv \frac{d_1 P}{a_1} \pmod{a_1}$, so we have $c_1 \equiv d_1 \pmod{a_1}$. Repeating this for all $i \in [1, n-1]$, we get $c_i \equiv d_i \pmod{a_i}$ for all $1 \le i \le n-1$.

Therefore, in order to get the maximum purple term $a_n \sum_{i=1}^{n-1} \frac{c_i \alpha}{a_i}$ with no purple terms above it, we need to set set $c_i = a_i - 1$ for all $1 \le i \le n-1$. The maximum purple term comes out to

$$a_n\alpha(n-1) - a_n\sum_{i=1}^{n-1}\frac{\alpha}{a_i} = (n-1)P - \sum_{i=1}^{n-1}\frac{P}{a_i},$$

and subtracting $\alpha = \frac{P}{a_n}$ gives the desired result. □

Remark 4.5. When $n = 2$, we recognize this as the well-known Chicken McNugget Theorem: the largest positive integer that cannot be expressed as a nonnegative integral linear combination of two relatively prime positive integers p, q is indeed $pq - p - q$.

Note that applying this lemma in the case where n is replaced with $n-1$ gives that the maximal nonelement of the numerical semigroup H is precisely

$$(n-2)\frac{P}{a_n} - \sum_{i=1}^{n-1}\frac{P}{a_n}a_i,$$

which is the term found in Lemma 4.3.

4.2 Calculating the difference in global minima of τ-sequences

Using Lemma 4.3 and our results about the Δ-function and τ-sequence in Section 3, we are now ready to prove Theorem 4.1.

Proof. Given a Seifert homology sphere $Y = \Sigma(a_1, a_2, \ldots, a_n)$, we define

$$t = \frac{1}{2}\left((n-2)\alpha - \sum_{i=1}^{n-1}\frac{\alpha}{a_i} + 1\right).$$

Also recall

$$N_0 = (n-2)a_1a_2\cdots a_n - \sum_{i=0}^{n}\frac{a_1a_2\cdots a_n}{a_i} = (2t-1)a_n - \alpha.$$

Denote $a_n' = a_n + \alpha$, and $Y' = \Sigma(a_1, a_2, \ldots, a_n')$.

Definition 4.6. We say that a blue bordered box sa_n is *greening* if $\Delta(sa_n) > 0$ (equivalently, $s \in H$). Otherwise, if $s \notin H$ and $\Delta(sa_n) \le 0$, we say that the blue bordered box sa_n is *reddening*. This is because these boxes are where the values of the Δ-function change color within the column.

Notice that for any cell x, at least one of #(greening borders nonstrictly above x) and #(reddening borders strictly below x) is zero (where above and below here refer to cells in the same column as x), and that the former minus the latter is equal to $\Delta(x)$.

Lemma 4.7. *We have that* $\chi(0) = -t$.

Proof. Note that $\chi(0) = \Delta(-\alpha) + \cdots + \Delta(-1)$. Since all negative numbers have nonpositive Δ values, $\chi(0)$ is equal to the total number of nonnegative reddening boxes, i.e. the number of nonnegative $s \notin H$. By Lemma 4.4, the maximal nonelement of H is

$$2t - 1 = (n-2)\alpha - \sum_{i=1}^{n-1} \frac{\alpha}{a_i}.$$

Furthermore, out of the $2t$ blue bordered numbers $0, a_n, 2a_n, \cdots, (2t-1)a_n$, exactly half are reddening. This is because by Theorem 3.1 (noting $N_0 + \alpha = (2t-1)a_n$),

$$1 = \Delta(sa_n) + (\Delta(N_0 - sa_n) + 1) = \Delta(sa_n) + \Delta((2t-1)a_n - sa_n),$$

so exactly one of sa_n and $(2t-1)a_n - sa_n$ are reddening. Hence there are exactly t nonnegative reddening boxes. □

Denote the Δ-functions of Y and Y' as $\Delta(\bullet)$ and $\Delta'(\bullet)$ respectively. Consider the grids (defined in Section 3) representing these two Δ-functions. Observe that the following transformation on the Δ grid turns it into the Δ' grid:

- Take each blue border, say around some number sa_n, and move it down s cells to the number $sa_n + s\alpha = sa'_n$.
- In addition, change the Δ values by stipulating that the Δ values inside each blue border remains the same (note we have $\Delta(sa_n) = \Delta'(sa'_n)$ since sa_n is primitive if and only if sa'_n is primitive). We then enforce Lemma 3.5, that the Δ values inside each cell is the same as the one above it, unless it has a blue border (in which case it's one greater).

The following important observation about χ is clear from Lemmas 3.6 and 4.7.

Lemma 4.8. *We have that*

1. $\chi(x) < 0$ *if* $x \le (t-1)a_n$,
2. $\chi(x) = 0$ *if* $(t-1)a_n + 1 < x \le ta_n$,
3. $\chi(x) > 0$ *if* $x > ta_n$.

This and the later Theorem 4.10 motivates the following definition:

Definition 4.9. We call the interval $((t-1)a_n - \alpha, (t-1)a_n]$ the *critical strip*. Note that the critical strip consists of the α consecutive numbers up to the $(t-1)$-th blue bordered box.

The critical strip two very important properties, given in the following two theorems.

Theorem 4.10. *The first occurrence of the global minimum* $\min_{x\geq 0} \tau(x)$ *of the* τ*-sequence occurs in the critical strip. That is, if* m *is the smallest positive integer such that* $\tau(m) = \min_{x\geq 0} \tau(x)$*, then* $m \in ((t-1)a_n - \alpha, (t-1)a_n]$.

Proof. Note that by Lemma 4.8, if $x \leq (t-1)a_n - \alpha$, then $\chi(x+\alpha) < 0$, so $\tau(x+\alpha) < \tau(x)$. In addition, if $x > (t-1)a_n$, then $\chi(x) \geq 0$, so $\tau(x-\alpha) \leq \tau(x)$. Therefore, the first occurrence of the global minimum of τ occurs in the critical strip. □

Theorem 4.11. *Under the grid transformation from* Δ *to* Δ'*, the values of the* Δ*- and* Δ'*-functions in the critical strips of their respective grids remains the same. This is equivalent to the color schemes of the* Δ *and* Δ' *grids being the same in their respective critical strips.*

Proof. Each blue border remains in its original column, and the relative ordering of the blue borders remains the same, so for any given cell in the critical strip, the quantity

$$\#(\text{greening border nonstrictly above}) - \#(\text{reddening border strictly below})$$

remains the same after the transformation from the Δ grid to the Δ' grid. □

In particular, this means that the first occurrence of the global minimum of the τ-sequence remains in the same position relative to the critical strip, so

$$\min_{x\geq 0} \tau_{Y'}(x) - \min_{x\geq 0} \tau_Y(x) = \sum_{x=0}^{(t-1)a'_n} \Delta'(x) - \sum_{x=0}^{(t-1)a_n} \Delta(x),$$

since $(t-1)a'_n$ and $(t-1)a_n$ are the endpoints of the critical strips of Y' and Y, respectively. Denote the interval $[0,(t-1)a_n]$ in the grid of Δ as $\mathcal{R}$, and similarly define $\mathcal{R}'$ for Δ' as the interval $[0,(t-1)a'_n]$.

Note that $\sum_{x=0}^{(t-1)a_n} \Delta(x)$ equals

$$\sum_{x=0}^{(t-1)a_n} \#(\text{greening borders nonstrictly above } x) - \#(\text{reddening borders strictly below } x)$$
$$= \sum_{\text{greening borders } g} \#(\text{cells nonstrictly below } g \text{ in } \mathcal{R})$$
$$- \sum_{\text{reddening borders } r} \#(\text{cells strictly above } r \text{ in } \mathcal{R}),$$

with a similar statement holding for $\sum_{x=0}^{(t-1)a'_n} \Delta'(x)$. Therefore, in order to compute the quantity

$$\sum_{x=0}^{(t-1)a'_n} \Delta'(x) - \sum_{x=0}^{(t-1)a_n} \Delta(x),$$

for each greening border sa_n we consider the change in its "contribution" to these sums before and after the transformation:

$$\begin{aligned}\delta(sa_n) := \#(&\text{cells in } \mathcal{R}' \text{ nonstrictly below } sa'_n)\\ &- \#(\text{cells in } \mathcal{R} \text{ nonstrictly below } sa_n).\end{aligned}$$

Similarly, for reddening borders sa_n we define

$$\begin{aligned}\delta(sa_n) := \#(&\text{cells in } \mathcal{R}' \text{ strictly above } sa'_n)\\ &- \#(\text{cells in } \mathcal{R} \text{ strictly above } sa_n).\end{aligned}$$

Therefore,

$$\sum_{x=0}^{(t-1)a'_n} \Delta'(x) - \sum_{x=0}^{(t-1)a_n} \Delta(x) = \sum_{sa_n \text{ is greening}} \delta(sa_n) - \sum_{sa_n \text{ is reddening}} \delta(sa_n).$$

We compute these two sums separately:

- Let there be ℓ greening borders in the $\mathcal{R}$ (hence there are $t-\ell$ reddening borders in the $\mathcal{R}$, since there are t total blue borders in the $\mathcal{R}$). For each of these greening borders sa_n, under the transformation it moves down by s cells, while the end of the critical strip moves down by $t-1$ cells. Hence $\delta(sa_n) = (t-1) - s$, so

$$\sum_{sa_n \text{ is greening}} \delta(sa_n) = (t-1)\ell - \sum_{sa_n \text{ in } \mathcal{R} \text{ is greening}} s.$$

- As proven in Lemma 4.7, there are exactly t nonnegative reddening boxes, and we noted above that $t-\ell$ of them are in $\mathcal{R}$. For any reddening box below $\mathcal{R}$ (there are ℓ of these), its contribution changes under the transformation by $t-1$ due to the critical strip moving downwards by $t-1$ cells. For any reddening box sa_n inside $\mathcal{R}$, it moves down by s cells, and hence its contribution changes by $\delta(sa_n) = s$. So

$$\sum_{sa_n \text{ is reddening}} \delta(sa_n) = (t-1)\ell + \sum_{sa_n \text{ in } \mathcal{R} \text{ is reddening}} s$$

Subtracting these two quantities, we obtain

$$\sum_{x=0}^{(t-1)a'_n} \Delta'(x) - \sum_{x=0}^{(t-1)a_n} \Delta(x) = -\sum_{\text{all } sa_n \text{ in } \mathcal{R}} s = -\frac{t(t-1)}{2}.$$

Substituting in our definition of t, we obtain exactly the condition that Lemma 4.3 requires in order to prove Theorem 4.1. $\square$

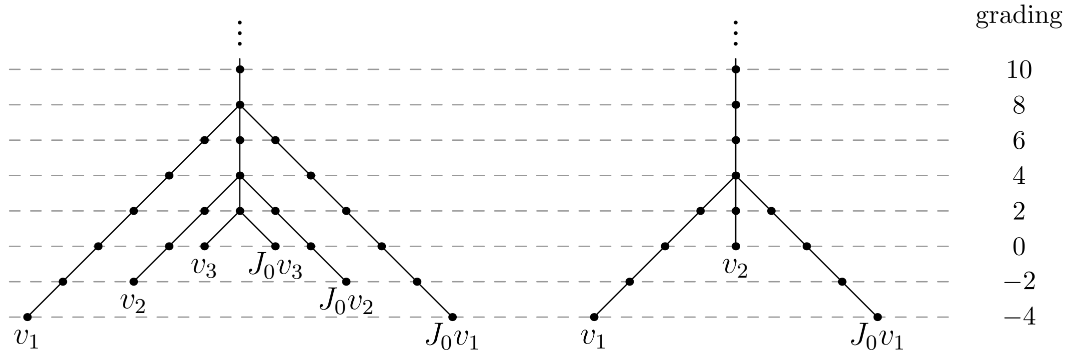

Figure 7: Two examples of monotone subroots. The left is the subroot $M(-4, 8; -2, 4; 0, 2)$ and the right is the subroot $M(-4, 4; 0, 0)$.

5 Results on Maximal Monotone Subroots

In this section, we define the *maximal monotone subroot* of a graded root lattice homology, which was introduced recently in [6]. This maximal monotone subroot is a *monotone graded root* which captures the general major structure of the graded root lattice homology.

First, we describe what a general monotone graded root is. Take a positive integer n and two sequences of rational numbers $h_1 < h_2 < \cdots < h_n$ and $r_1 > r_2 > \cdots > r_n$ such that they all differ from each other by even integers and $h_n \leq r_n$. To construct the root, we first form the stem with lowermost grading r_n by drawing an infinite tower upwards from a vertex at height r_n on the page. Then, for each $1 \leq i < n$, we draw a pair of vertices v_i and J_0v_i at grading h_i, where J_0v_i is the vertex v_i reflected over the vertical axis of the graded root. We then connect them to the stem at grading r_i. If $h_n > r_n$, we introduce a similar pair of vertices v_n and J_0v_n. Otherwise, $v_n = J_0v_n$ at grading r_n. This constructs the monotone subroot $M = M(h_1, r_1; \ldots; h_n, r_n)$. Two examples are shown in Figure 7.

Now, we define the maximal monotone subroot of a lattice homology graded root. The maximal monotone subroot is defined by starting at the smallest (most negative) grading and then greedily traveling up the stem, adding branches to the subroot if their tips have strictly lower grading than any previous tips. More precisely, define the following terminology: for any node v we define the infinite tower extending upwards from v as γ_v, and denote the first point at which γ_v meets the stem as $b(v)$, called the *base* of v. The cluster C_b based at some grading b consists of all vertices with base b. The tips of a cluster are the pair of vertices in it with minimal grading (if there is more than one such pair symmetrical about the stem, we arbitrarily select one of the pairs. If the size of C_b is 1 we just select the stem vertex at grading b). Now to construct the maximal monotone subroot, we start at the vertex on the stem with the smallest grading (say with grading r), and add the tips of C_r to the subroot. Then we move to the vertex on the stem with the next smallest grading (travelling up the stem), and add the tips of its cluster to the subroot if and only if those tips have strictly smaller grading than any previously added tips. This process continues until at some point all the clusters we consider are trivial (i.e. consist of a single vertex on the stem). This must eventually happen because the number of clusters is finite in any graded root resulting from a lattice homology (for example, because the τ-extrema sequence

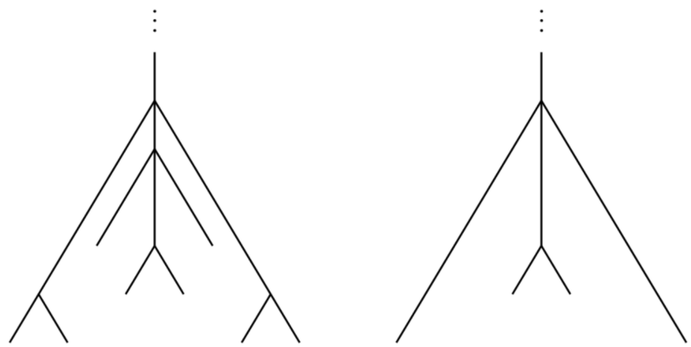

Figure 8: A graded root on the left and its maximal monotone subroot on the right.

is finite since no local extrema exist outside of $[0, N_0]$). An example of a graded root and its maximal monotone subroot is shown in Figure 8.

Maximal monotone subroots have high importance in relation to the graded roots of the lattice homologies of 3-manifolds, such as in the study of homology cobordism. First, we state the following helpful lemma, which is evident from the definition of the τ-sequence and maximal monotone subroot.

Lemma 5.1. *For any pair of symmetric global minima $\tau(m)$ and $\tau(N_0 - m)$ of the τ-sequence, the maximal monotone subroot is fully determined by the values of the Δ-function in the interval $[m, N_0 - m]$, up to a shift in grading.*

Theorem 5.2. *The maximal monotone subroots of the lattice homologies of the Seifert homology spheres $Y = \Sigma(a_1, a_2, \dots, a_n)$ and $Y'' = \Sigma(a_1, a_2, \dots, a_n + 2\alpha)$ are the same.*

Proof. Denote $a_n'' := a_n + 2\alpha$. We will show that there is a pair of global minima $\tau_Y(m)$ and $\tau_Y(N_0 - m)$ of τ_Y and a pair of global minima $\tau_{Y''}(m'')$ and $\tau_{Y''}(N_0'' - m'')$ of $\tau_{Y''}$ such that the values of τ_Y on the interval $[m, N_0 - m]$ and the values of $\tau_{Y''}$ on the interval $[m'', N_0'' - m'']$ are identical, which finishes.

As shown in Section 4, the first global minimum of τ_Y must occur in the critical strip $((t-1)a_n - \alpha, (t-1)a_n]$. Since the Δ-function is antisymmetric under the map $x \mapsto N_0 - x$ by Theorem 3.1, we have that that τ-sequence is symmetric under that map. In particular, the last global minimum of τ_Y must occur in the region

$$[N_0 - (t-1)a_n, N_0 - (t-1)a_n + \alpha) = [ta_n - \alpha, ta_n),$$

which is the image of the critical strip under this map. Now note that the region $((t-1)a_n - \alpha, ta_n)$ contains two symmetric global minima and corresponds to a centrally symmetric region of the graded root of Y (since the endpoints $(t-1)a_n - \alpha$ and ta_n sum to N_0). By Lemma 5.1, we can fully determine the monotone subroot (up to a shift in the grading) solely based on the Δ values in that region.

The corresponding region in Y'' is $((t-1)a_n'' - \alpha, ta_n'')$, but the length of this interval is too long. Instead, we will consider the interval

$$((t-1)a_n'', ta_n'' - \alpha),$$

which is a centrally symmetric region of the graded root of Y'', and that the length of this interval is the same as that of $((t-1)a_n - \alpha, ta_n)$.

By Lemma 5.1, it suffices to show that the sequence of Δ values within the interval $((t-1)a_n - \alpha, ta_n)$ are exactly the same as the Δ'' values within the interval $((t-1)a''_n, ta''_n - \alpha)$, since these sequences fully determine the maximal monotone subroots of the lattice homologies Y and Y'', respectively. Indeed, for any $0 < i < a_n + \alpha$ we have

$$\Delta((t-1)a_n - \alpha + i) = \Delta''((t-1)a''_n - \alpha + i) = \Delta''((t-1)a''_n + i)$$

where the first equality holds due to our discussion in Section 4 about the transformation from Δ to Δ' (and then to Δ''), and the second equality follows from Lemma 3.5 since $(t-1)a''_n + i$ is never a multiple of a''_n. Thus, the monotone subroots of Y and Y'' are the same up to a shift in grading.

In addition, Theorem 4.1 guarantees that the d-invariants are the same, so the grading of the global minima of Y and Y'' are the same. In conclusion, the maximal monotone subroots of the lattice homologies of Y and Y'' are identical. $\square$

6 Future Work

In the future, we would like to attempt to resolve other questions about Seifert fibered integral homology spheres as they relate to lattice homology. For example, we would eventually like to compute the Heegaard-Floer Homology of all Seifert fibered integral homology spheres through their lattice homology, but we hypothesize this cannot be done for some time.

In terms of the work in this paper, we are mainly interested in exploring what happens to the maximal monotone subroot of the lattice homology of a Seifert fibered integral homology $\Sigma(a_1, a_2, \dots, a_n)$ when we add $a_1 a_2 \cdots a_{n-1}$ to the last term. We conjecture that, in the 3-fiber case, the monotone subroot will always change under this transformation unless the Brieskorn sphere features small p, q, r (such as $\Sigma(2,3,5)$ or $\Sigma(2,3,7)$); perhaps the monotone subroot only remains the same under this transformation when the lattice homology is weakly elliptic. However, more numerical testing and mathematical work is needed to resolve this.

Some other subproblems we are interested in include proving rank inequalities dealing with the lengths of towers in the lattice homology graded root of Seifert fibered integral homology spheres, in the style of or extending the work in [15]. We are also interested in developing a faster algorithm for computing the lattice homology of larger plumbed 3-manifolds, as the algorithm provided in Section 2 is very slow for even plumbings with 10-15 vertices.

7 Acknowledgements

We would like to thank our mentor Dr. Irving Dai for his guidance throughout the project as well as the MIT PRIMES program under which this research was conducted. All team members contributed to all aspects of the project.

References

[1] Selman Akbulut and Kyle Larson. Brieskorn spheres bounding rational balls. *Proceedings of the American Mathematical Society*, 146(4):1817–1824, 2018.

[2] Maciej Borodzik and András Némethi. Heegaard–floer homologies of (+ 1) surgeries on torus knots. *Acta Mathematica Hungarica*, 139(4):303–319, 2013.

[3] Valentin Bosshard. Lagrangian cobordisms in liouville manifolds. *arXiv preprint arXiv:2105.14821*, 2021.

[4] Mahir B Can and Çagrı Karakurt. Calculating heegaard–floer homology by counting lattice points in tetrahedra. *Acta Mathematica Hungarica*, 144(1):43–75, 2014.

[5] Tim Cochran and Daniel Tanner. Homology cobordism and seifert fibered 3-manifolds. *Proceedings of the American Mathematical Society*, 142(11):4015–4024, 2014.

[6] Irving Dai and Ciprian Manolescu. Involutive heegaard floer homology and plumbed three-manifolds. *J. Inst. Math. Jussieu*, 18(6):1115–1155, 2019.

[7] J Fernández de Bobadilla, I Pallarés, and M Saito. Hodge modules and cobordism classes. *arXiv preprint arXiv:2103.04836*, 2021.

[8] Margaret Doig and Stephan Wehrli. A combinatorial proof of the homology cobordism classification of lens spaces. *arXiv preprint arXiv:1505.06970*, 2015.

[9] Selahi Durusoy. Heegaard-floer homology and a family of brieskorn spheres. *arXiv preprint math/0405524*, 2004.

[10] Ronald Fintushel and Ronald J Stern. Instanton homology of seifert fibred homology three spheres. *Proceedings of the London Mathematical Society*, 3(1):109–137, 1990.

[11] Kristen Hendricks, Jennifer Hom, Matthew Stoffregen, and Ian Zemke. Surgery exact triangles in involutive heegaard floer homology. *arXiv preprint arXiv:2011.00113*, 2020.

[12] Kristen Hendricks, Ciprian Manolescu, and Ian Zemke. A connected sum formula for involutive heegaard floer homology. *Selecta Mathematica*, 24(2):1183–1245, 2018.

[13] Jennifer Hom. Heegaard floer homology, lectures 1–4. 2019.

[14] Jennifer Hom. Homology cobordism, knot concordance, and heegaard floer homology. *arXiv preprint arXiv:2108.10400*, 2021.

[15] Çağrı Karakurt and Tye Lidman. Rank inequalities for the heegaard floer homology of seifert homology spheres. *Trans. Am. Math. Soc.*, 367(10):7291–7322, 2015.

[16] Tye Lidman and Eamonn Tweedy. A note on concordance properties of fibers in seifert homology spheres. *Can. Math. Bull.*, 61(4):754–767, 2018.

[17] Ciprian Manolescu. Homology cobordism and triangulations. In *Proceedings of the International Congress of Mathematicians: Rio de Janeiro 2018*, pages 1175–1191. World Scientific, 2018.

[18] András Némethi. On the ozsváth-szabó invariant of negative definite plumbed 3-manifolds. *Geometry & Topology*, 9(2):991–1042, 2005.

[19] András Némethi. Lattice cohomology of normal surface singularities. *Publications of the Research Institute for Mathematical Sciences*, 44(2):507–543, 2008.

[20] William E Olsen. Trisections and ozsvath-szabo cobordism invariants. *arXiv preprint arXiv:2102.00910*, 2021.

[21] Peter Ozsváth and Zoltán Szabó. On the floer homology of plumbed three-manifolds. *Geometry & Topology*, 7(1):185–224, 2003.

[22] Peter Ozsváth and Zoltán Szabó. Holomorphic disks and topological invariants for closed three-manifolds. *Annals of Mathematics*, pages 1027–1158, 2004.

[23] Peter Ozsváth and Zoltán Szabó. An introduction to heegaard floer homology. *Floer homology, gauge theory, and low-dimensional topology*, 5:3–27, 2006.

[24] Nikolai Saveliev. Floer homology of brieskorn homology spheres. *J. Differ. Geom.*, 53(1):15–87, 1999.

[25] R Dale Shipp. Table of dedekind sums. *J. Res. Nut. Bur. Standavds Sect. B*, 69:259–263, 1965.

[26] Jan Steinebrunner. The classifying space of the one-dimensional bordism category and a cobordism model for tc of spaces. *Journal of Topology*, 14(1):62–111, 2021.

[27] Eamonn Tweedy. Heegaard floer homology and several families of brieskorn spheres. *Topol. Appl.*, 160(4):620–632, 2013.

Declaration of Academic Integrity

The participating team declares that the paper submitted is comprised of original research and results obtained under the guidance of the instructor. To the team's best knowledge, the paper does not contain research results, published or not, from a person who is not a team member, except for the content listed in the references and the acknowledgment. If there is any misinformation, we are willing to take all the related responsibilities.

Names of team members: Karthik Seetharaman, William Yue, Isaac Zhu

Signatures of team members:

Karthik Seetharaman:

William Yue:

Isaac Zhu:

Name of the instructor: Dr. Irving Dai

Signature of the instructor:

Date: 09/13/21